Photocatalytic Initiation of Radical Thiol-Ene Reactions Using Carbon-Bi_2O_3 Nanocomposites

Viviana Maffeis,[†,‡] *Ruairí O. McCourt,*[§] *Rita Petracca,*[§] *Olivier Laethem,*[§] *Adalberto Camisasca,*[†,‡] *Paula E. Colavita*[§]* *Silvia Giordani*[†,¶]* *and Eoin M. Scanlan*[§]*

[†]Nano Carbon Materials, Istituto Italiano di Tecnologia (IIT), Via Livorno 60, 10144 Turin, Italy.

[‡]Department of Chemistry and Industrial Chemistry, University of Genoa, via Dodecaneso 31, Genoa, 16145, Italy.

[§]School of Chemistry and Trinity Biomedical Sciences Institute (TBSI), Trinity College Dublin, The University of Dublin, Dublin 2, Ireland.

[¶]Department of Chemistry, University of Turin, Via Giuria 7, 10125 Turin, Italy.

KEYWORDS: Thiol-ene, radical, photocatalysis, graphene, nanomaterials, metal oxide

ABSTRACT: A mild, inexpensive and general photocatalytic initiation protocol for anti-Markovnikov hydrothiolation of olefins using carbon nanomaterial/metal oxide (Carbon NM-MO) composites is reported. Graphene oxide (GO), nanodiamonds (ND) and carbon nano-onions (CNO) displaying bismuth or tungsten oxide nanoparticles adhered to the surface, function as highly efficient photocatalysts for thiol-ene ligation under both UV and visible-light-mediated

conditions. The straightforward catalyst preparation, excellent overall yields, ease of purification and broad substrate scope render this a highly versatile method for bioconjugation.

Introduction

Thiyl-radical mediated reactions are widely utilized in nature for a range of essential biochemical processes.[1] Cysteinyl residues play a key role as reactive species in many enzymatic pathways including the deoxygenation of ribonucleotides in the *de novo* synthesis of DNA precursors.[2-3] The broad application of thiyl radicals in biological processes arises from their exceptional reactivity and chemoselectivity. It is therefore not surprising that thiyl-radical mediated reactions have been harnessed by synthetic chemists for a diverse range of chemical transformations.[1, 4] Thiol-ene ligation is widely utilized for the formation of carbon-sulfur bonds in chemical synthesis[5-10], catalysis[4], bioconjugation[11-12], polymerisation[13-15] and surface modification.[16] The process is cytocompatible[17] and adheres to the concept of a *'click'* reaction as defined by Sharpless in 2001.[18] Radical thiol-ene ligation reactions are typically carried out under UV conditions in the presence of a radical initiator such as 2,2-dimethoxy-2-phenyl-acetophenone (DPAP).[1, 7] Recently, visible-light-mediated photoredox catalysis has emerged as a convenient alternative to UV initiation, allowing for greater substrate compatability.[19-25] Yoon and co-workers demonstrated efficient thiol–ene reactions under photoredox conditions using ruthenium catalysts with visible light.[23-24] Stephenson and co-workers reported a similar strategy for radical thiol-ene coupling in which a trichloromethyl radical genereated *via* single-electron reduction of bromotrichloromethane acted as a radical chain carrier.[21] Recently, metal oxides such as

TiO_2 or BiO_3 have been investigated as catalysts for thiol-ene ligation, however the requirement for stoichiometric quantities of the metal oxide or the addition of chain carrier reagents such as $BrCCl_3$ render these methods unsuitable for certain biological applications[20] (Figure 1). Despite the bourgeoning interest in photocatalysed thiol-ene ligation, the application of carbon nanomaterials (CNMs) remains unexplored. It is known that highly efficient photocatalysts can be prepared as composite semi-conducting materials composed of metal oxides adhered to the surface of carbon nanomaterials.[26-29] These low-cost photocatalysts have been investigated for environmental applications including water purification.[30-31] Carbon carbon nanomaterial/metal oxide (NM-MO) composites are readily prepared through a number of methods including the simple stirring of the two materials at room temperature.[32] The carbon NM-MO composite offers a synergic effect induced by the presence of carbon materials in the hybrid photocatalyst.[33] This is mainly attributed to the decrease of electron/hole recombination, bandgap tuning and increase in the adsorptive active sites.[34] Herein we present the application of both CNMs and carbon NM-MO composites as highly-efficient photocatalysts for light-mediated thiol-ene ligation reactions. Characterisation of the composite materials is presented and a putative mechanism for the catalytic cycle is depicted. Substrate scope is explored across inter- and intramolecular thiol-ene ligation and intermolecular thiol-yne reactions. Of particular note is the short reaction times, quantitative yields and ease of purification of the products.

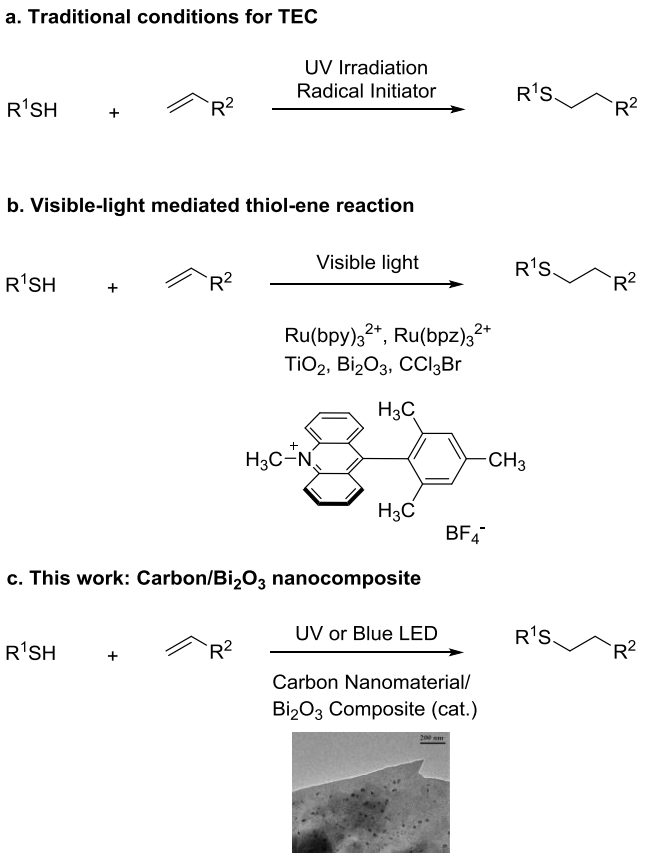

Figure 1: Pathway for photocatalysed thiol-ene ligation reactions (a) conventional UV mediated conditions (b) visible-light mediated catalysts (c) overview of catalyst described herein.

Results and discussion

The utility of Bi_2O_3 as a photocatalyst in visible-light-mediated thiol-ene ligation was reported by Pfizer as part of a methodology development effort.[35] However, the metal oxide alone was found to be an inefficient photocatalyst for thiol-ene coupling (TEC) and $BrCCl_3$ was added as a chain carrier. Bi_2O_3, which possesses a bandgap of 2.6-2.8 eV[36] (477-442 nm), is a well-studied metal oxide semiconductor, but its efficiency as a photocatalyst is often low because of the rapid recombination of the photo-generated electrons and holes.[35] We set out to investigate if the photocatalytic properties of Bi_2O_3

could be enhanced in a non-toxic and environmentally benign manner through the use of carbon material/Bi_2O_3 nano-composites. In our initial studies, the TEC between allyl benzoate and thioacetic acid was investigated as a model system to screen suitable photocatalysts. A range of carbon nanomaterials were screened for TEC in the presence of a metal oxide. The results of these initial screening studies are presented in Table 1. It was determined that all of the nanomaterials screened, when combined with Bi_2O_3 (2 mol%) or WO_3 (2 mol%), resulted in the complete conversion of the starting allyl benzoate **1** into the desired thioester **2** under UV irradiation after 1 hour (Table 1, entries 1-10). These promising results showed that the photocatalytic activity was general across the range of carbon nanomaterial/metal oxide composites investigated. Absorption of compounds **1** and **2** is negligible in the region >320 nm; therefore, under the reaction conditions used, photocatalysis can only result from photoexcitation of the composite nano materials. Interestingly, the nanomaterials in the absence of any metal oxide were also able to propagate the radical reaction, albeit without full conversion to the thioester (Table 1, entries 11-15). Overall good conversions, varying from 65% (p-CNO, entry 12) to 94% (PEG-CNO, entry 14), were determined for all the screened nanomaterials. That the metal oxide was required for full conversion to the desired thioester product suggests a synergic effect induced through the combination of carbon nanomaterials and metal oxide in the hybrid photocatalysts (see proposed mechanism).

Table 1. Nanomaterials screened for the thiol−ene ligation reaction of allyl benzoate with thioacetic acid.

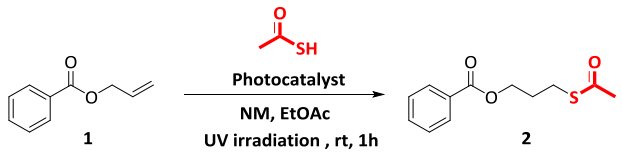

Entry	**NM**	Photocatalyst	**2** Yield (%)[b]
1	**ND**	Bi_2O_3	**>99**
2	**p-CNO**	Bi_2O_3	**>99**
3	**Ox-CNO**	Bi_2O_3	**>99**
4	**PEG-CNO**	Bi_2O_3	**>99**
5	**GO**	Bi_2O_3	**>99**
6	**ND**	WO_3	**>99**
7	**p-CNO**	WO_3	**>99**
8	**Ox-CNO**	WO_3	**>99**
9	**PEG-CNO**	WO_3	**>99**
10	**GO**	WO_3	**>99**
11	**ND**	-	89
12	**p-CNO**	-	65
13	**Ox-CNO**	-	70
14	**PEG-CNO**	-	94
15	**GO**	-	84

NM = nanomaterials; **ND** = nanodiamonds; **CNO** = carbonanoonions; **GO** = graphene oxide; [a]Reactions were conducted by irradiating allyl benzoate **1** (0.5 mmol), thioacetic acid (2.0 mmol), the NM (10 mg/mL, 7 µl) and the photocatalyst (0.02 equiv) in degassed EtOAc (0.7 mL) with 365 nm lamps for 1 h. [b] ^{1}H-NMR conversion.

Following the success of the model studies, we set out to investigate the effect of catalyst loading on the yield of the thiol-ene ligation. In this study, the nanocomposite was freshly prepared prior to addition to the thiol-ene ligation reaction. Preparation of the nanocomposite involved a two-step protocol whereby the carbon nanomaterial and metal

oxide were first sonicated together in EtOAc and subsequently filtered through a nylon syringe filter (pore size 1 μm) in order to remove large particles, resulting in an optically transparent dispersion of the photocatalytic nanocomposite. In the case of the GO- and CNO-Bi_2O_3 nanocomposites, the material was fully characterised using a range of techniques and determined to be composed of bismuth oxide nanoparticles adhered to the surface of the carbon nanomaterial (see materials characterisation). Varying volumes of the CNO-MO composites were added to the thiol-ene reaction (Table 2, entries 1-4), until complete conversion into the desired thioester was achieved (Table 2, entry 4). The possible contribution/participation of water in the radical reaction was investigated by varying the water concentration under identical reaction conditions. The use of the dry ethyl acetate (Table 2, entry 4) did not result in any significant change in yield compared to when a wet solvent was employed (Table 2, entry 5). On the contrary, the addition of a small amount of water (100 μL) led to a decrease in the product conversion (Table 2, entry 6). Once the optimal reaction conditions for a fast and complete thioester conversion were established with CNOs, we also tested the commercially available graphene oxide (GO) as the carbon component of the nanocomposite. As reported in Table 2, entry 7, the GO-Bi_2O_3 nanocomposite was efficient in delivering full conversion of the thiol-ene ligation. The crude ^{1}H-NMR of the reaction mixture after 1 h, without any aqueous work-up, is shown in Figure 2 and demonstrates the efficacy of the photocatalytic process. This finding is significant since both GO and Bi_2O_3 are cheap, commercially available materials. Furthermore the ease of removal of these reagents upon aqueous work-up is ideal for synthetic chemistry.

Table 2. Carbon NM-MO composites screened at varying volumes of addition.

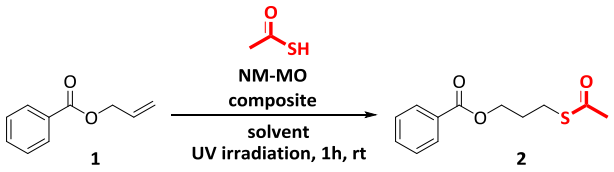

Entry	NM	NM/Bi_2O_3 composite	solvent	**2** Yield (%)[b]
1	**Ox-CNO**	10 µg/mL	EtOAc	90
2	**Ox-CNO**	20 µg/mL	EtOAc	91
3	**Ox-CNO**	40 µg/mL	EtOAc	92
4	**Ox-CNO**	80 µg/mL	EtOAc	**>99**
5	**Ox-CNO**	80 µg/mL	EtOAc (dry)	**>99**
6	**Ox-CNO**	80 µg/mL	EtOAc (+H_2O)	39
7	**GO**	80 µg/mL	EtOAc	**>99**

CNO = carbon nanoonions; **GO** = graphene oxide; [a]Reactions were conducted by irradiating allyl benzoate **1** (0.5 mmol), thioacetic acid (2.0 mmol) and the NM-MO composite (56 µl) in degassed EtOAc (0.7 mL) with 365 nm lamps for 1 h. [b] ^{1}H-NMR conversion.

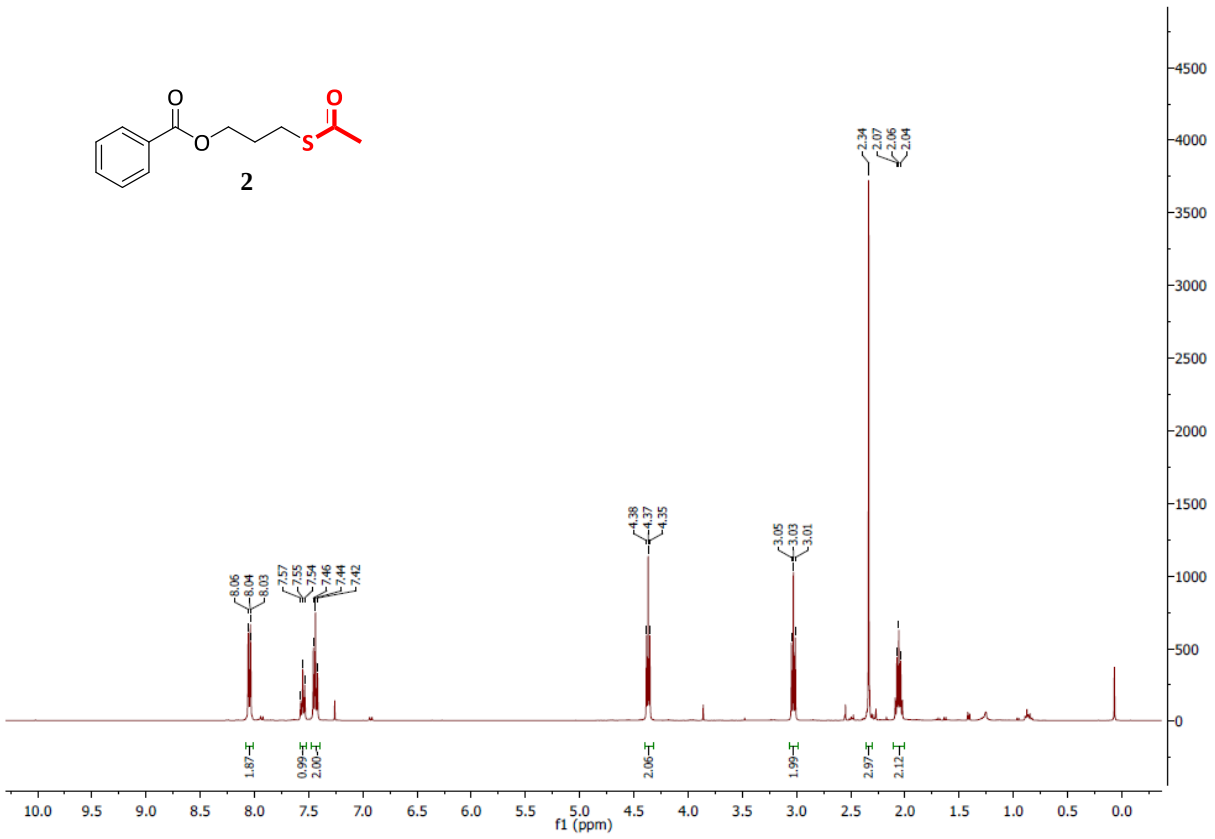

Figure 2: 600 MHz ^{1}H-NMR spectrum of crude ligation product **2** after photolysis in degassed EtOAc for 1 h in the presence of GO-Bi_2O_3 (Table 2, Entry 7).

In order to investigate the scope of our catalytic approach, the thiol-ene ligation reaction was also carried out under visible-light-mediated initiation using blue-LEDs (Table 3). In general, very good conversion values were obtained for all the screened nanomaterial composites, although, in contrast to the UV mediated process, no full-conversion could be obtained (Table 3, entries 1-5). When the nanocomposite concentration was increased up to 80 µg/mL, with both Ox-CNO (entry 6) and GO (entry 7), a slightly higher yield was achieved. It is possible that further tuning of the nanomaterial composition would render the visible-light-mediated process as efficient as the UV reaction.

Table 3. Carbon NM-MO composites screened for the thiol-ene ligation under visible-light-mediated conditions.

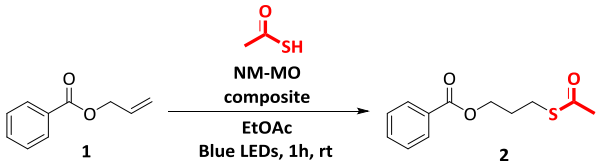

Entry	**NM/Bi_2O_3 composite**	**2** Yield (%)[b]
1	**ND** (10 µg/mL)	90
2	**p-CNO** (10 µg/mL)	79
3	**Ox-CNO** (10 µg/mL)	70
4	**PEG-CNO** (10 µg/mL)	78
5	**GO** (10 µg/mL)	71
6	**Ox-CNO** (80 µg/mL)	79
7	**GO** (80 µg/mL)	78
8	**GO** (80 µg/mL), 3 h	80

NM = nanomaterial; **ND** = nanodiamonds; **CNO** = carbon nanoonions; **GO** = graphene oxide; [a]Reactions were conducted by irradiating allyl benzoate **1** (0.5 mmol), thioacetic acid (2.0 mmol) and the NM-MO (56 µl), in degassed EtOAc (0.7 mL) with 405 nm lamps for 1 h. [b1]H-NMR conversion.

With the optimized photocatalytic conditions in hand, we set out to investigate the scope and limitations of the nanocomposite for TEC across a broad variety of thiols and alkenes. As depicted in Figure 3, all the TEC products were obtained in high isolated yields. Both thioacids and alkylthiols were compatible with the photocatalytic process to furnish thioesters and thioethers. Boc-protected cysteine derivatives **5**, **7** and the peracetylated thiosugars **8**, **9** demonstrated the compatibility of the nanocomposite catalytic approach with the preparation of bioconjugates. The GO-Bi_2O_3 nanocomposite was also extremely

efficient in catalysing the thiol-yne ligation with the dual-addition product **11a** formed in 58% and the corresponding mono-addition product **11b** isolated in 35%. In addition, we also investigated the nanocomposites as photocatalysts for the intramolecular thiol-ene process to furnish **10**. This fast cyclisation process offers access to unique families of sulfur containing heterocycles including thiosugars.[37-39] Of particular importance in these synthetic studies was the ease of purification of the products which could be achieved through simple filtration. This offers a significant advantage over the traditional DPAP/MAP initiated processes, where extensive column chromatography is required to seperate the product from the degraded initiator and photosensitizer. In addition, no discolouration of the reaction mixture was observed during either the UV or visible-light-mediated photolysis, ensuring that the photoinitiation was not compromised at any point. This is a major advantage over previously reported processes where milligram quantities of metal oxide are utilized and strong discolouration and precipitation of metal oxides is observed.

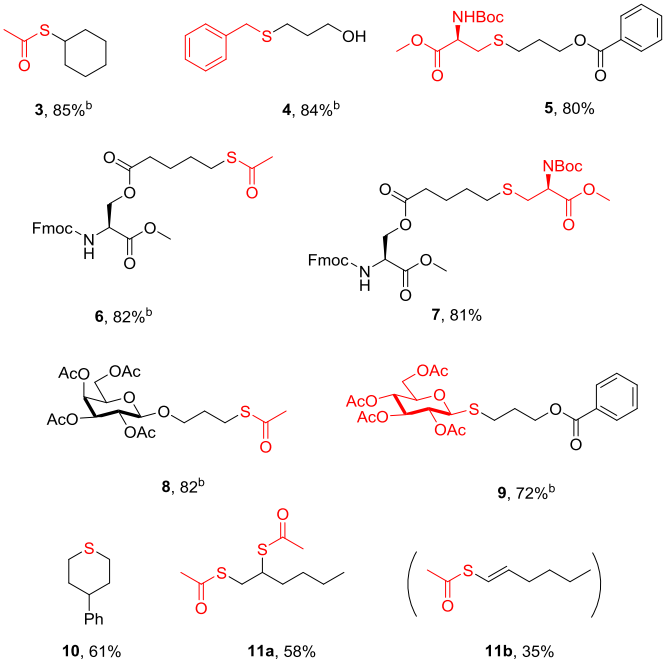

[a]Reactions were conducted by irradiating alkene (1 equiv.), thiol (4 equiv. with the exception of compounds **9** and **10** where 1.5 equiv. was used), NM-MO (composite with Bi_2O_3), (56 µl) in EtOAc (0.7 mL) with 365 nm lamps for 1 h; [b]Isolated yield.

Figure 3: Carbon NM-MO catalysed thiol-ene ligation, expansion of synthetic scope.

Materials Characterization

The morphology and crystallography of the GO-Bi_2O_3 and CNO-Bi_2O_3 samples was characterized by transmission electron microscopy (TEM). Bright-field TEM imaging of the Bi_2O_3/ox-CNO composite and Bi_2O_3/GO composite was performed on a Jeol JEM-1011 instrument equipped with a thermoionic tungsten source operated at 100 kV. Samples were prepared by spreading a droplet of the dispersed composite material in ethanol on a copper grid coated with a lacey carbon film. Figure 4A shows a TEM image of Bi_2O_3 nanoparticles, which display mainly a spherical shape with a size ranging from 10 to 20 nm. Figure 4B shows a TEM image of GO, which displays the typical transparent paper-like structure of GO with a lateral size of about 1 µm and around 15-18 layers, which is in agreement with the Sigma-Aldrich specifications. Interestingly, in comparison with the TEM image of graphene nanosheets, the TEM image of the Bi_2O_3/GO composites (Figure 4C) shows that the surface of the graphene–bismuth oxide composite is much rougher than that of graphene nanosheets. This observation may be attributed to the presence of bismuth oxide nanoparticles on graphene sheets. Moreover, the TEM images suggest that the bismuth oxide nanoparticles (about 10nm in size) are uniformly distributed on 2D graphene nanosheets (Figure 4C). Similarly, TEM images of the ox-CNO composite material show homogenous black spots arrayed on the ox-CNO

surfaces, a feature quite different in respect to the smooth ox-CNO with size ranging from 20 to 40 nm (Figure 4D). For both composites, TEM images indicate that the catalyst is well dispersed and attached to the graphene oxide and to the oxidized carbon nano-onion surfaces. In the Powder X-ray diffraction pattern (XRD) of the Bi_2O_3 oxide, the main peaks match the reflections, respectively, characteristic of the α-Bi_2O_3 polymorph (Supporting Information).

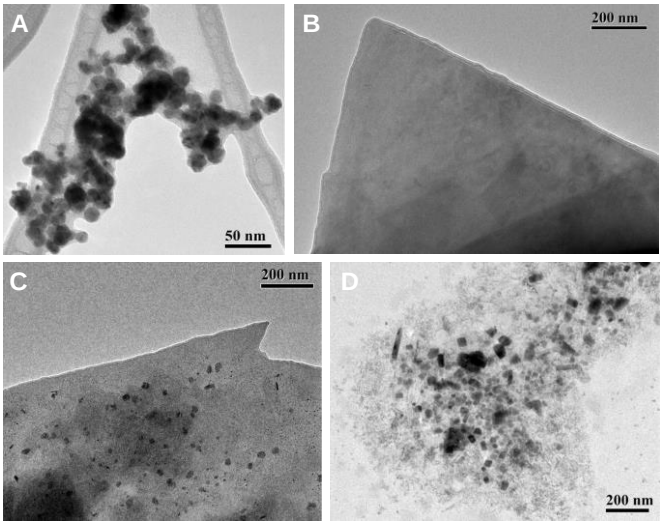

Figure 4. TEM images of (A) Bi_2O_3 nanoparticles; (B) GO nanosheets; (C) Bi_2O_3/GO nanocomposite; and (D) Bi_2O_3/ox-CNO composite.

Proposed Mechanism

A proposed mechanism for the overall photocatalytic process is outlined in Scheme 1. Bi_2O_3 has a bandgap of 2.6-2.8 eV and a conduction band edge at -4.8 eV vs. vacuum (i.e. +0.4 eV vs. NHE).[40] Pristine few layer graphene has a zero bandgap and a work function (WF) of 4.2 eV;[41] however the presence of oxidised groups can result in an increase in WF of up to ~2 eV and the creation of localized states within the π-π^* gap.[42] XPS analysis of Bi_2O_3 showed no discernible change after exposure to UV for 1 h suggesting

no other oxides are formed under these conditions (ESI S3 and S4). Scheme 1 shows the position of semiconductor levels relative to those of a generic graphene oxide material. Considering that oxidation of alkylthiols and thioacetic acid are observed at $E°(RS,H^+/RSH)$ = 1.3-1.7 V_{NHE}[43] and $E°(AcS,H^+/AcSH)$ = 1.4 V_{NHE},[44] it is clear from the scheme that photoexcitation of Bi_2O_3 can result in the direct oxidation of RSH species by photogenerated holes to form thiyl radicals and protons (eqn. 1)

$$RSH + h^+ \rightarrow RS^{\bullet} + H^+ \qquad \text{(eqn. 1)}$$

Organosulfides are in fact well known to act as substrates for the direct reaction of photogenerated holes in the case of TiO_2 photooxidative processes.[45] The thiyl radical initiates the TEC process through anti-Markovnikov addition onto an alkene and generation of an alkyl radical, which propagates the reaction by abstracting a hydrogen atom from the starting thiol (Scheme 2). High concentrations of $RS^{\bullet}$ radical initiators are desirable for achieving fast thiol-ene reaction rates, and these should be facilitated by (a) removal of competing reductants and (b) long hole lifetimes. In the presence of water, reactions compete with water oxidation so that lower thiol-ene reaction efficiencies in water-rich solutions should be expected. This is in agreement with observed trends in reaction yields after the use of dry and water-spiked EtOAc as solvent in our experiments (Table 2; entry 4 and 6). UV and blue excitations used in our experiments can be absorbed by both Bi_2O_3 and the carbon nanomaterials, however, the presence of a composite in which the oxide and the carbon material are in intimate contact results in high reaction efficiencies. This suggests that the two materials function in synergy and a likely explanation is that the composite improves charge separation and reduces h-e recombination rates. The addition of carbon nanomaterials has been explored as a strategy

for enhancing photoconversion yields of semiconductor particles. Most notably, coupling of TiO_2 to a range of carbon nanomaterials has been widely explored for oxidative degradation of organics,[46] and enhancements have been observed with oxides such as WO_3[47] and $BiVO_4$.[48] The enhancement mechanism remains under debate and hypotheses include[46] the transfer of conduction band electrons from the oxide to carbon acceptor states which can be further enhanced by optical excitation of the carbon nanomaterial.

The first report of Bi_2O_3 catalyzed thiol-ene reactions leveraged the photoinduced reductive cleavage of an organohalide ($BrCCl_3$) for the generation of the radical initiator.[35] In the case of our work no initiator is needed for the reaction to go to completion, while the addition of carbon as an electron trapping agent appears essential. In the light of this finding it is interesting to speculate whether the role of the organobromide in carbon-free reactions is that of acting as both a radical initiator and an electron trap, as proposed for similar reactions of other organohalides.[49]

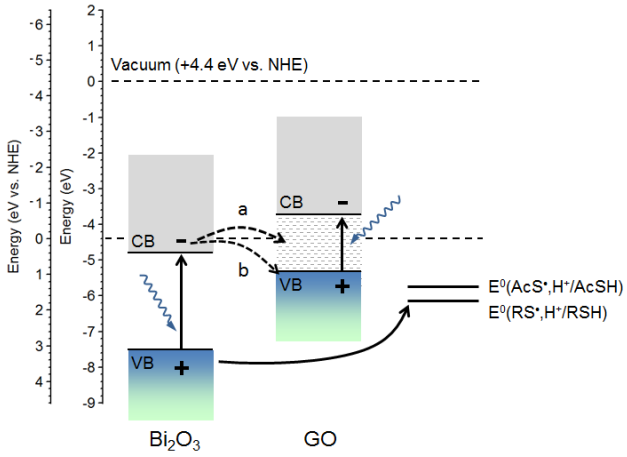

Scheme 1. (a) Conduction (CB) and valence band (VB) edges of Bi_2O_3 and of a generic graphene oxide (GO) nanomaterial, and their relative alignment with respect to the standard

redox potentials of alkylthiols and thioacetic acid. Photoexcited electrons in the CB of Bi_2O_3 can be trapped e.g. by local states (path a) or by holes in the VB of photoexcited GO (path b).

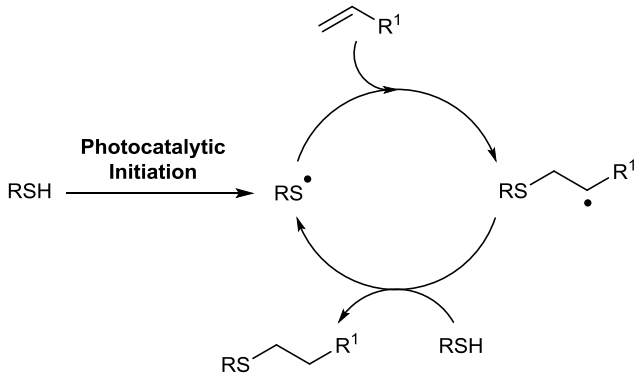

Scheme 2. Thiol-ene reaction propagation following photocatalytic initiation by the metal oxide-nanomaterial nanocomposite.

Conclusions

We have developed an efficient, robust and readily accessible general photocatalytic process for the thiol-ene *'click'* reaction. The use of metal oxide-carbon nanocomposites renders the process highly efficient for photocatalysis. The process appears to be general for a wide range of ligation reactions including, inter- and intramolecular thiol-ene, and thiol-yne ligation. The nanomaterials were fully characterised as bismuth oxide nanoparticles adhered to the surface of the carbon nanomaterials, and a putative reaction mechanism for the catalytic cycle is presented. The simple catalyst preparation, high-yields, ease of purification and biocompatibility render this a highly attractive option for cytocompatible thiol-ene ligation reactions.

Supporting Information

The Supporting Information is available free of charge on the ACS Publications website at DOI:xxxxx

Experimental procedures for nanocomposites preparation, Bright-field TEM of Bi_2O_3 - ox-CNO/GO nanocomposites, XPS of Bi_2O_3, ^{1}H- and ^{13}C-NMR Spectra of thioether and thioester products.

AUTHOR INFORMATION

Corresponding Authors

* Tel.: +353-1-8962514. E-mail: eoin.scanlan@tcd.ie, s.giordani@unito.it, colavitp@tcd.ie

Orchid

Eoin M. Scanlan 0000-0001-5176-2310

Ruairí O. McCourt 0000-0002-3237-7764

Author Contributions

The manuscript was written through contributions of all authors. All authors have given approval to the final version of the manuscript.

Notes

The authors declare no competing financial interest.

ACKNOWLEDGMENT

This work was supported by Science Foundation Ireland (SFI) under grant number 15/CDA/3310 (E. M. S., R. P.); Istituto Italiano di Tecnologia (V. M., A. C., S. G.) and by a philanthropic donation to Trinity College Dublin by Beate Schuler (R. O. M.).

ABBREVIATIONS

TEC, Thiol-ene 'click'; NM, nanomaterials; ND, nanodiamonds; CNO, carbonanoonions; p-CNO, pristine carbonanoonions; GO, graphene oxide;

REFERENCES

1. Denes, F.; Pichowicz, M.; Povie, G.; Renaud, P., Thiyl radicals in organic synthesis. *Chem. Rev.* **2014,** *114*, 2587-2693.
2. Kolberg, M.; Strand, K. R.; Graff, P.; Kristoffer Andersson, K., Structure, function, and mechanism of ribonucleotide reductases. *Biochimica et Biophysica Acta, Proteins and Proteomics* **2004,** *1699*, 1-34.
3. Fontecave, M., Ribonucleotide reductases and radical reactions. *Cellular and Molecular Life Sciences* **1998,** *54*, 684-695.
4. Hashimoto, T.; Kawamata, Y.; Maruoka, K., An organic thiyl radical catalyst for enantioselective cyclization. *Nature Chemistry* **2014,** *6*, 702-705.
5. Hoyle, C. E.; Bowman, C. N., Thiol-Ene Click Chemistry. *Angewandte Chemie, International Edition* **2010,** *49*, 1540-1573.
6. McCourt, R. O.; Denes, F.; Sanchez-Sanz, G.; Scanlan, E. M., Rapid Access to Thiolactone Derivatives through Radical-Mediated Acyl Thiol-Ene and Acyl Thiol-Yne Cyclization. *Organic Letters* **2018,** *20*, 2948-2951.
7. Markey, L.; Giordani, S.; Scanlan, E. M., Native chemical ligation, thiol-ene Click: A methodology for the synthesis of functionalized peptides. *Journal of Organic Chemistry* **2013,** *78*, 4270-4277.
8. Li, L.; Liu, H., Rapid Preparation of Silsesquioxane-Based Ionic Liquids. *Chemistry - A European Journal* **2016,** *22*, 4713-4716.
9. Li, L.; Xue, L.; Feng, S.; Liu, H., Functionalization of monovinyl substituted octasilsesquioxane via photochemical thiol-ene reaction. *Inorganica Chimica Acta* **2013,** *407*, 269-273.
10. Li, L.; Feng, S.; Liu, H., Hybrid lanthanide complexes based on a novel β-diketone functionalized polyhedral oligomeric silsesquioxane (POSS) and their nanocomposites with PMMA via in situ polymerization. *RSC Advances* **2014,** *4*, 39132-39139.
11. Floyd, N.; Vijayakrishnan, B.; Koeppe, J. R.; Davis, B. G., Thiyl Glycosylation of Olefinic Proteins: S-Linked Glycoconjugate Synthesis. *Angewandte Chemie, International Edition* **2009,** *48*, 7798-7802, S7798/1-S7798/72.
12. Dondoni, A.; Massi, A.; Nanni, P.; Roda, A., A New Ligation Strategy for Peptide and Protein Glycosylation: Photoinduced Thiol-Ene Coupling. *Chemistry--A European Journal* **2009,** *15* (43), 11444-11449.
13. Espeel, P.; Du Prez, F. E., One-pot multi-step reactions based on thiolactone chemistry: A powerful synthetic tool in polymer science. *Eur. Polym. J.* **2015,** *62*, 247-272.
14. Fairbanks, B. D.; Love, D. M.; Bowman, C. N., Efficient Polymer-Polymer Conjugation via Thiol-ene Click Reaction. *Macromolecular Chemistry and Physics* **2017,** *218*.
15. Tunca, U., Orthogonal multiple click reactions in synthetic polymer chemistry. *Journal of Polymer Science, Part A: Polymer Chemistry* **2014,** *52*, 3147-3165.
16. Gupta, N.; Lin, B. F.; Campos, L. M.; Dimitriou, M. D.; Hikita, S. T.; Treat, N. D.; Tirrell, M. V.; Clegg, D. O.; Kramer, E. J.; Hawker, C. J., A versatile approach to high-throughput microarrays using thiol-ene chemistry. *Nature Chemistry* **2010,** *2*, 138-145.
17. DeForest, C. A.; Anseth, K. S., Cytocompatible click-based hydrogels with dynamically tunable properties through orthogonal photoconjugation and photocleavage reactions. *Nature Chemistry* **2011,** *3*, 925-931.

18. Kolb, H. C.; Finn, M. G.; Sharpless, K. B., Click chemistry: diverse chemical function from a few good reactions. *Angewandte Chemie, International Edition* **2001,** *40*, 2004-2021.
19. Zhao, G.; Kaur, S.; Wang, T., Visible-Light-Mediated Thiol-Ene Reactions through Organic Photoredox Catalysis. *Organic Letters* **2017,** *19*, 3291-3294.
20. Bhat, V. T.; Duspara, P. A.; Seo, S.; Abu Bakar, N. S. B.; Greaney, M. F., Visible light promoted thiol-ene reactions using titanium dioxide. *Chemical Communications* **2015,** *51*, 4383-4385.
21. Keylor, M. H.; Park, J. E.; Wallentin, C.-J.; Stephenson, C. R. J., Photocatalytic initiation of thiol-ene reactions: synthesis of thiomorpholin-3-ones. *Tetrahedron* **2014,** *70*, 4264-4269.
22. Limnios, D.; Kokotos, C. G., Photoinitiated Thiol-Ene ''Click'' Reaction: An Organocatalytic Alternative. *Advanced Synthesis & Catalysis* **2017,** *359*, 323-328.
23. Tyson, E. L.; Ament, M. S.; Yoon, T. P., Transition metal photoredox catalysis of radical thiol-ene reactions. *Journal of Organic Chemistry* **2013,** *78*, 2046-2050.
24. Tyson, E. L.; Niemeyer, Z. L.; Yoon, T. P., Redox Mediators in Visible Light Photocatalysis: Photocatalytic Radical Thiol-Ene Additions. *Journal of Organic Chemistry* **2014,** *79*, 1427-1436.
25. Wimmer, A.; Konig, B., Photocatalytic formation of carbon-sulfur bonds. *Beilstein journal of organic chemistry* **2018,** *14*, 54-83.
26. Zhang, H.; Lv, X.-J.; Li, Y.-M.; Wang, Y.; Li, J.-H., P25-Graphene Composite as a High Performance Photocatalyst. *ACS Nano* **2010,** *4*, 380-386.
27. Sun, L.; Zhao, Z.; Zhou, Y.; Liu, L., Anatase TiO2 nanocrystals with exposed {001} facets on graphene sheets via molecular grafting for enhanced photocatalytic activity. *Nanoscale* **2012,** *4*, 613-20.
28. Zhong, J.; Chen, F.; Zhang, J., Carbon-Deposited TiO2: Synthesis, Characterization, and Visible Photocatalytic Performance. *Journal of Physical Chemistry C* **2010,** *114*, 933-939.
29. Xiang, Q.; Yu, J.; Jaroniec, M., Synergetic effect of MoS2 and graphene as cocatalysts for enhanced photocatalytic H2 production activity of TiO2 nanoparticles. *J Am Chem Soc* **2012,** *134*, 6575-8.
30. Li, L.; Wang, M., Advanced nanomatericals for solar photocatalysis. *Advanced Catalytic Materials* **2016**, 169-230.
31. Ye, A.; Fan, W.; Zhang, Q.; Deng, W.; Wang, Y., CdS-graphene and CdS-CNT nanocomposites as visible-light photocatalysts for hydrogen evolution and organic dye degradation. *Catalysis Science & Technology* **2012,** *2*, 969-978.
32. Frederick, R. T.; Novotny, Z.; Netzer, F. P.; Herman, G. S.; Dohnalek, Z., Growth and Stability of Titanium Dioxide Nanoclusters on Graphene/Ru(0001). *Journal of Physical Chemistry B* **2017**, Ahead of Print.
33. Bell, N. J.; Ng, Y. H.; Du, A.; Coster, H.; Smith, S. C.; Amal, R., Understanding the Enhancement in Photoelectrochemical Properties of Photocatalytically Prepared TiO2-Reduced Graphene Oxide Composite. *Journal of Physical Chemistry C* **2011,** *115*, 6004-6009.
34. Geng, W.; Liu, H.; Yao, X., Enhanced photocatalytic properties of titania-graphene nanocomposites: a density functional theory study. *Physical Chemistry Chemical Physics* **2013,** *15*, 6025-6033.
35. Fadeyi Olugbeminiyi, O.; Mousseau James, J.; Feng, Y.; Allais, C.; Nuhant, P.; Chen Ming, Z.; Pierce, B.; Robinson, R., Visible-Light-Driven Photocatalytic Initiation of Radical Thiol-Ene Reactions Using Bismuth Oxide. *Org Lett* **2015,** *17*, 5756-9.
36. Strehlow, W. H.; Cook, E. L., Compilation of energy band gaps in elemental and binary compound semiconductors and insulators. *Journal of Physical and Chemical Reference Data* **1973,** *2*, 163-99.
37. Corce, V.; McSweeney, L.; Malone, A.; Scanlan, E. M., Intramolecular thiol-yne cyclization as a novel strategy for thioglycal synthesis. *Chemical Communications* **2015,** *51*, 8672-8674.
38. Malone, A.; Scanlan, E. M., Applications of Thiyl Radical Cyclizations for the Synthesis of Thiosugars. *Organic Letters* **2013,** *15*, 504-507.
39. Scanlan, E. M.; Corce, V.; Malone, A., Synthetic applications of intramolecular thiol-ene "click" reactions. *Molecules* **2014,** *19*, 19137-19151, 15 pp.
40. Xu, Y.; Schoonen, M. A. A., The absolute energy positions of conduction and valence bands of selected semiconducting minerals. *American Mineralogist* **2000,** *85*, 543-556.
41. Garg, R.; Dutta, N. K.; Choudhury, N. R., Work function engineering of graphene. *Nanomaterials* **2014,** *4*, 267-300, 34 pp.
42. Kumar, P. V.; Bernardi, M.; Grossman, J. C., The Impact of Functionalization on the Stability, Work Function, and Photoluminescence of Reduced Graphene Oxide. *ACS Nano* **2013,** *7*, 1638-1645.
43. Surdhar, P. S.; Armstrong, D. A., Reduction potentials and exchange reactions of thiyl radicals and disulfide anion radicals. *Journal of Physical Chemistry* **1987,** *91*, 6532-7.
44. Zhao, R.; Lind, J.; Merenyi, G.; Eriksen, T. E., One-Electron Reduction Potential and the β-Fragmentation of Acetylthiyl Radical, Comparisons with Benzoylthiyl Radical and the Oxygen Counterparts. *Journal of Physical Chemistry A* **1999,** *103*, 71-74.

45. Vorontsov, A. V., Photocatalytic transformations of organic sulfur compounds and H2S. *Russian Chemical Reviews* **2008,** *77*, 909-926.
46. Leary, R.; Westwood, A., Carbonaceous nanomaterials for the enhancement of TiO2 photocatalysis. *Carbon* **2011,** *49*, 741-772.
47. Gomis-Berenguer, A.; Celorrio, V.; Iniesta, J.; Fermin, D. J.; Ania, C. O., Nanoporous carbon/WO3 anodes for an enhanced water photooxidation. *Carbon* **2016,** *108*, 471-479.
48. Wang, T.; Li, C.; Ji, J.; Wei, Y.; Zhang, P.; Wang, S.; Fan, X.; Gong, J., Reduced Graphene Oxide (rGO)/BiVO4 Composites with Maximized Interfacial Coupling for Visible Lght Photocatalysis. *ACS Sustainable Chemistry & Engineering* **2014,** *2*, 2253-2258.
49. Colavita, P. E.; Streifer, J. A.; Sun, B.; Wang, X.; Warf, P.; Hamers, R. J., Enhancement of Photochemical Grafting of Terminal Alkenes at Surfaces via Molecular Mediators: The Role of Surface-Bound Electron Acceptors. *Journal of Physical Chemistry C* **2008,** *112* (13), 5102-5112.